Generalized nonequilibrium vertex correction method in coherent medium theory for quantum transport simulation of disordered nanoelectronics

Jiawei Yan and Youqi Ke[*]

Division of Condensed Matter Physics and Photonic Science,
School of Physical Science and Technology, ShanghaiTech University, Shanghai 201210, China

Electron transport properties of nanoelectronics can be significantly influenced by the inevitable and randomly distributed impurities/defects. For theoretical simulation of disordered nanoscale electronics, one is interested in both the configurationally averaged transport property and its statistical fluctuation that tells device-to-device variability induced by disorder. However, due to the lack of an effective method to do disorder averaging under the nonequilibrium condition, the important effects of disorders on electron transport remain largely unexplored or poorly understood. In this work, we report a general formalism of Green's function based nonequilibrium effective medium theory to calculate the disordered nanoelectronics. In this method, based on a generalized coherent potential approximation for the Keldysh nonequilibrium Green's function, we developed a generalized nonequilibrium vertex correction method to calculate the average of a two-Keldysh-Green's-function correlator. We obtain nine nonequilibrium vertex correction terms, as a complete family, to express the average of any two-Green's-function correlator and find they can be solved by a set of linear equations. As an important result, the averaged nonequilibrium density matrix, averaged current, disorder-induced current fluctuation, and averaged shot noise, which involve different two-Green's-function correlators, can all be derived and computed in an effective and unified way. To test the general applicability of this method, we applied it to compute the transmission coefficient and its fluctuation with a square-lattice tight-binding model and compared with the exact results and other previously proposed approximations. Our results show very good agreement with the exact results for a wide range of disorder concentrations and energies. In addition, to incorporate with density functional theory to realize first-principles quantum transport simulation, we have also derived a general form of conditionally averaged nonequilibrium Green's function for multicomponent disorders.

I. INTRODUCTION

Due to experimental imperfections or doping for special functionality, disordered impurities/defects are inevitable in realistic nanoelectronic devices. The disorders can significantly influence or even completely determine the quantum transport properties of the device [1–3] and give rise to large device-to-device variability on the nanometer scale [4,5]. Thus, thorough understanding of the effects of disorders is critically important for both modern device technology and fundamental transport physics. However, quantum transport simulation of disordered nanoelectronics faces several difficulties: (i) since electron transport in current flow is an intrinsically nonequilibrium process, the nonequilibrium quantum statistics must be correctly treated in the simulation; (ii) the strong coupling of transport properties to the atomic, chemical, and materials details at the nanoscale requires accurate atomic-level simulation without using any empirical parameter; (iii) the absence of translational invariance in disordered devices renders many well established state-of-the-art computational methods useless; (iv) the theoretical transport property, such as current, must be averaged over a large ensemble of disorder configurations to be physically meaningful; (v) for the nanoscale device, the device-to-device variability induced by disorders is a general and important phenomenon and it is thus important to calculate the statistical fluctuation of the transport property. Since these difficulties involve different areas of physics, one must combine different theoretical algorithms together to realize the simulation of disordered nanoelectronics. As far as we know, the above five difficulties have only been partially solved; no general algorithm has been reported to calculate disordered nanoelectronics. To solve the first two difficulties, the present workhorse for simulation of nanoelectronics combines the nonequilibrium (NE) Green's function (GF) method [6–8] with density functional theory (DFT) [9–11] to account for nonequilibrium statistics from first principles. (Implementation examples are Refs. [12–21].) However, the applicability of the NEGF-DFT method is limited to perfect or ordered nanoelectronics. The remaining three difficulties are basically related to how to do disorder averaging to obtain averaged nonequilibrium electronic structure, transport property, and its fluctuation. Recently, considerable efforts have been devoted to addressing the disorder averaging problem in the NEGF framework and incorporating with the DFT method to simulate disordered nanoelectronics. In Ref. [22], one of the authors (Y.K.) and his coworkers have applied a conventional coherent potential approximation (CPA) [23,24] to construct a translational invariant effective medium to compute the averaged retarded/advanced GF $G^{R/A}$ and then developed a nonequilibrium vertex correction (NVC) method to obtain the averaged NEGF $\langle G^{<} \rangle = \langle G^{R} \Sigma^{<} G^{A} \rangle = \langle G^{R} \rangle (\Sigma^{<} + \Omega_{NVC}) \langle G^{A} \rangle$ (where $\Sigma^{<}$ is the lesser self-energy of electrodes and Ω_{NVC} is the NVC). In this method, the NVC accounts for not only effects of the multiple impurity scattering, but also the

---
*[*]keyq@shanghaitech.edu.cn

nonequilibrium quantum statistics, for which it is named. In combination with the NEGF-DFT quantum transport method, the CPA-NVC has seen important applications in simulating nanoelectronics with atomic disorders [22,25–34]. Besides, an alternative approach called nonequilibrium CPA (NECPA) has been reported independently in Refs. [35,36]. In this method, the CPA is generalized to treat the configurational average of the contour-ordered Green's function to obtain the $\langle G^< \rangle$ by introducing a nonequilibrium coherent potential. Although NECPA provides a different derivation of $\langle G^< \rangle$, Ref. [36] proves that the nonequilibrium coherent potential in NECPA and the NVC are the same quantity within the single-site approximation in the CPA. Because the CPA-NVC or NECPA developed so far can only calculate the average of a single NEGF, namely $\langle G^< \rangle$, the present available methods only allow the calculation of nonequilibrium electronic structure and averaged electron current. However, other properties require the average of the two-NEGF correlator; for example, the disorder-induced current fluctuation and averaged quantum shot noise contain $\langle G^< C G^< \rangle$ as we will show in Sec. II, representing a great challenge for the present available methods. By rewriting $\langle G^< C G^< \rangle = \langle G^R \Sigma^< G^A C G^R \Sigma^< G^A \rangle$, several different approximations have been proposed to compute the average of this quantity which involves the complex four-Green's-function correlator. For example, Ref. [37] reported a perturbation expansion method and Ref. [5] reported a low concentration limit approximation and a Green's function based diagrammatic technique. However, these approximate methods [5,37] are not generally applicable. In particular, the perturbation expansion [37] and low concentration limit approximation [5] may only be valid for the case of low concentration and weak scattering, and the diagrammatic technique as reported [5] can give large errors and even generate unphysical results. Therefore, we can see there is no general algorithm that allows the computation of both the $\langle G^< \rangle$ and $\langle G^< C G^< \rangle$, and the simulation of disorder effects in nanoelectronics still requires further significant development in quantum transport theory.

In this paper, we report a generalized CPA-NVC algorithm to calculate the $\langle G^< \rangle$ and $\langle G^< C G^< \rangle$ in a unified and effective way, so that various transport properties of disordered nanoelectronics can be simulated. In this method, based on a generalized CPA for the Keldysh GF, the generalized NVC algorithm is developed to calculate the average of any two-Green's-function correlator, such as $\langle G^R C G^A \rangle$, $\langle G^< C G^< \rangle$, and other pairwise combinations of various Green's functions. We obtained nine generalized NVCs, which can be solved by a set of linear equations, to account for the effects of multiple impurity scattering under the nonequilibrium condition. With the nine generalized NVCs, the disorder-averaged nonequilibrium density matrix and various important transport properties, including averaged current, disorder-induced current fluctuation, and the averaged shot noise, can all be effectively computed. To test the general applicability of this method, we applied it to calculate the transmission coefficient and its fluctuation with a tight-binding model on a square lattice, and compared with the exact results and other previously proposed approximations [5]. Our calculations agree very well with the exact results for a wide range of disorder concentrations and energies, while other methods do not. In addition, to combine with

the DFT, a general form of the conditionally averaged NEGF $\langle G^{<,Q} \rangle$ is derived for multicomponent disorders (beyond the binary case reported in the previous CPA-NVC paper [22]) to do first-principles simulation of disordered nanoelectronics. The generalized CPA-NVC provides a unified, effective, and general method for simulation of electron transport properties of disordered nanoelectronics.

The rest of the paper is organized as follows. In Sec. II, we review the GF-based quantum transport method and we show that various disorder-averaged quantum transport properties can all be expressed in terms of two-GF correlators for disordered nanoelectronics. Section III reviews the various types of NEGFs and their relations, and the associated perturbation expansion technique. Section IV describes a generalized coherent medium theory to compute the average of the Keldysh GF. Section V formulates the generalized NVC method to calculate any two-GF correlator. In Sec. VI, we applied the generalized CPA-NVC method to calculate the averaged transmission and its fluctuation using a tight-binding model and compared our results with the exact calculations and other approximations. Section VII derives the general form of conditionally averaged NEGFs for multicomponent disorders to combine with DFT to realize first-principles simulations. Finally, we conclude in Sec. VIII and provide additional details in Appendices A, B, C, D, and E.

II. QUANTUM TRANSPORT PROPERTIES OF A DISORDERED DEVICE

In this section, we briefly review the NEGF-based quantum transport theory. We only consider a two-probe device as shown in Fig. 1(a).

The central scattering region containing the disordered impurities is sandwiched by two semi-infinite ideal leads. Under a finite bias, electrons flow from one lead to the other with scattering events happening on the disordered impurities. The electron-photon, electron-phonon interactions are not considered in this paper, but in principle, they can be taken into account in the NEGF formalism [8,38]. Since the two-probe device shown in Fig. 1(a) is infinite and nonperiodic in the
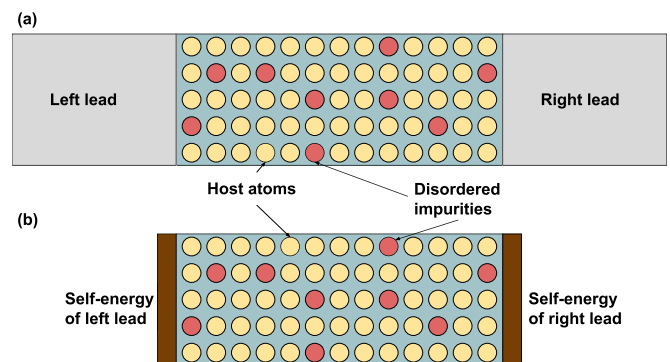
FIG. 1. Physical model for a two-probe nanoelectronic device with disorders. (a) The central device region with disorders is sandwiched by two semi-infinite leads. (b) The effects of the leads are turned into the self-energies so that the central device region becomes calculable.

transport direction, it cannot be calculated directly. We usually turn the effects of the two semi-infinite leads into the lead self-energies Σ_{ld}, as shown in Fig. 1(b), so that the central device region becomes calculable.

For simplicity, we here only give some important results for quantum transport properties within the NEGF theory, and more details can be found in the related literature [7,39]. The retarded GF, G^R, is directly associated with the Hamiltonian of the central device region H through

$$G^R = \left[E - H - \Sigma_{ld}^R \right]^{-1}, \qquad (1)$$

where $\Sigma_{ld}^R = \Sigma_L^R + \Sigma_R^R$ is the retarded self-energy due to the left and right leads. The advanced GF and self-energy are conjugate with the retarded ones, namely $G^A = [G^R]^\dagger$ and $\Sigma_{ld}^A = [\Sigma_{ld}^R]^\dagger$. Since we assume the leads will not be affected by the scattering region, Σ_{ld} is a constant, independent of the disorder in the central device region. For the device shown in Fig. 1, the averaged nonequilibrium electron density of the central region is given by

$$\langle \rho(\mathbf{r}) \rangle = -i \int \frac{dE}{2\pi} \langle G^<(\mathbf{r}, \mathbf{r}'; E) \rangle_{\mathbf{r}'=\mathbf{r}}, \qquad (2)$$

where $\langle G^< \rangle$ is the averaged lesser Green's function that can be calculated by the Keldysh formula

$$\langle G^< \rangle = \langle G^R \Sigma_{ld}^< G^A \rangle. \qquad (3)$$

Here, $\Sigma_{ld}^<$ is the lesser self-energy of the leads. It should be mentioned that we have dropped the boundary term in Eq. (3), which accounts for the contribution of bound states [40] and can be generally neglected for devices in the steady state that we are focusing on here [7]. Since the leads are in equilibrium states, we can get

$$\Sigma_{ld}^< = i[f_L(E)\Gamma_L + f_R(E)\Gamma_R], \qquad (4)$$

where $f_{L/R}(E)$ are the Fermi-Dirac distribution of the left and right leads. $\Gamma_{L/R}$ in Eq. (4) are called linewidth functions defined as $\Gamma_{L/R} \equiv i[\Sigma_{L/R}^R - \Sigma_{L/R}^A]$, describing the coupling between the scattering region and the leads. If we assume $f_L(E) = 1$ and $f_R(E) = 0$ at nonequilibrium, then Eq. (4) is reduced to

$$\Sigma_{ld}^<(E) = i\Gamma_L(E), \qquad (5)$$

where $\Gamma_L(E)$ is constant, independently of the disordered central region. From the Landauer-Büttiker formula [7], the averaged current through the device can be written as

$$\langle I \rangle = \int \frac{dE}{2\pi} \langle T(E) \rangle [f_L(E) - f_R(E)], \qquad (6)$$

where $\langle T(E) \rangle$ is the averaged transmission coefficient

$$\langle T(E) \rangle = \text{Tr}\langle G^R \Gamma_L G^A \Gamma_R \rangle. \qquad (7)$$

The current fluctuation δI under low bias can be approximated by [5]

$$\delta I \approx \int \frac{dE}{2\pi} \delta T(E) [f_L(E) - f_R(E)], \qquad (8)$$

where the transmission fluctuation is defined as $\delta T = \sqrt{\langle T^2 \rangle - \langle T \rangle^2}$, which requires the average of T^2. By writing

$\langle T^2 \rangle$ explicitly, we have

$$\begin{aligned} \langle T^2 \rangle &= \langle \text{Tr}[G^R \Gamma_L G^A \Gamma_R] \text{Tr}[G^R \Gamma_L G^A \Gamma_R] \rangle \\ &= -\langle \text{Tr}[G^< \Gamma_R] \text{Tr}[G^< \Gamma_R] \rangle, \end{aligned} \qquad (9)$$

where we have used Eqs. (3) and (5). This equation requires us to average a product of two traces, which is inconvenient in calculation. To go further, we make a decomposition[40] $\Gamma_R = \sum_i |W_i\rangle\langle W_i|$, where $|W_i\rangle$ is the normalized eigenvector of Γ_R. By putting this decomposed Γ_R into Eq. (9) and using the cyclic invariance property of the trace, we obtain

$$\langle T^2 \rangle = -\sum_i \sum_j \text{Tr}\langle G^< S_{ij} G^< S_{ij}^\dagger \rangle, \qquad (10)$$

where $S_{ij} \equiv |W_i\rangle\langle W_j|$ is independent of disorders. Additionally, the quantum shot noise [41,42] given as

$$\begin{aligned} \langle S \rangle = &\int \frac{dE}{\pi} \text{Tr}\langle \hat{T} \rangle [f_L(1 - f_L) + f_R(1 - f_R)] \\ &+ \int \frac{dE}{\pi} \text{Tr}[\langle \hat{T} \rangle - \langle \hat{T}^2 \rangle](f_L - f_R)^2 \end{aligned} \qquad (11)$$

where $\hat{T} \equiv G^R \Gamma_L G^A \Gamma_R$ called transmission operator, also involves the product of two lesser GFs.

At this point, we have seen that many physical quantities in electron transport, including the averaged nonequilibrium electron density, averaged current, current fluctuation, and shot noise, can all be expressed in terms of two-GF correlators, such as Eqs. (3), (7), and (10). In the following sections, we will discuss how to calculate the average of these two-GF correlators to realize the nonequilibrium transport simulation of disordered devices.

III. THE NONEQUILIBRIUM GREEN'S FUNCTION THEORY

We have introduced several kinds of GFs to express the quantum transport properties of nanoelectronics. In this section, we will briefly introduce the relations between various GFs and the different quantity representations in the NEGF theory and discuss the associated perturbation expansion technique.

A. Quantity representation in NEGF theory

The central quantity in the NEGF theory is the contour-ordered GF which is defined as [8]

$$G(\mathbf{r}, t; \mathbf{r}', t') \equiv -i\langle \Phi_0 | T_C[\psi_H(\mathbf{r}, t)\psi_H^\dagger(\mathbf{r}', t')] | \Phi_0 \rangle, \qquad (12)$$

where ψ_H is the field operator defined in the Heisenberg picture, and $\psi_H^\dagger$ is its conjugate. $|\Phi_0\rangle$ refers to the normalized ground state of the system. T_C is the contour-ordering operator that arranges the time-dependent operators according to their order on the time contour, which starts from remote past, passes through t and t', and finally returns to the remote past again, as shown in Fig. 2(a). The reason why the contour looks this way is because we are considering the nonequilibrium process, in which we cannot predict the system when $t \to +\infty$.

The same as the contour-ordered GF, in the NEGF theory, many other physical quantities, such as the Hamiltonian H, self-energy Σ, potential V, and T matrix T introduced in next
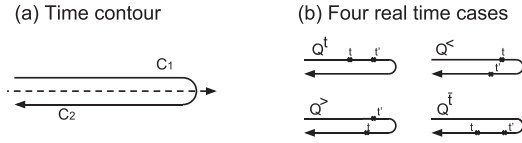
FIG. 2. (a) The time contour starts from $-\infty$, passes through t and t', and finally returns to $-\infty$. (b) Four possible combinations of t and t' on the time contour.

section, denoted as Q, can be defined on the time contour. For these contour-ordered quantities, the two time labels can lie on either of the two branches C_1 and C_2 on the contour as shown in Fig. 2(b). As a result, each contour-ordered quantity contains four different possibilities given as follows:

$$Q(t,t') = \begin{cases} Q^t(t,t') & t \in C_1, t' \in C_1, \\ Q^<(t,t') & t \in C_1, t' \in C_2, \\ Q^>(t,t') & t \in C_2, t' \in C_1, \\ Q^{\bar{t}}(t,t') & t \in C_2, t' \in C_2, \end{cases} \quad (13)$$

which are called time-ordered, lesser, greater, and anti-time-ordered real-time quantities, respectively. One can check that these four real-time quantities are not linearly independent since they satisfy $Q^t + Q^{\bar{t}} = Q^< + Q^>$ [38]. Conventionally, one can define another three real-time quantities [43]:

$$Q^R = Q^t - Q^< = Q^> - Q^{\bar{t}}, \quad (14)$$

$$Q^A = Q^t - Q^> = Q^< - Q^{\bar{t}}, \quad (15)$$

$$Q^K = Q^t + Q^{\bar{t}} = Q^> + Q^<. \quad (16)$$

These three terms are called retarded, advanced, and Keldysh quantities and have the relations $Q^R = [Q^A]^\dagger$ and $Q^K = -[Q^K]^\dagger$. If Q is Hermitian, then $Q^K = 0$ and $Q^R = Q^A$.

With the help of these real-time quantities, the contour-ordered quantity can be alternatively represented by using a 2×2 real-time matrix defined in the following form, as suggested by Craig [44]:

$$Q = \begin{pmatrix} Q^t & -Q^< \\ Q^> & -Q^{\bar{t}} \end{pmatrix}, \quad (17)$$

which contains the same amount of information as the time-contour representation. Since the four elements in the above matrix are not linearly independent, to eliminate this redundance, one can apply the Keldysh linear transformation $Q' = R^{-1}QR$ to the Craig matrix, where $R \equiv \frac{1}{\sqrt{2}} \begin{pmatrix} 1 & 1 \\ -1 & 1 \end{pmatrix}$ [6]. After the transformation, we get the Keldysh 2×2 matrix [6]

$$Q' = \begin{pmatrix} Q^A & 0 \\ Q^K & Q^R \end{pmatrix}, \quad (18)$$

where the relations in Eqs. (14), (15), and (16) are used. Note that the Keldysh matrix features a lower triangular matrix; the matrix addition, multiplication, and inverse operations on Keldysh matrices do not change the mathematical structure. Moreover, the zero element in Eq. (18) can greatly simplify the matrix operations. For these reasons, it is convenient to work in the Keldysh representation, and then make the transformation to the Craig matrix to obtain all the real-time GFs in Eq. (17).

As shown in Appendix A, one can assert the equivalence of using different representations of contour-ordered quantity in applications, including Craig/Keldysh real-time matrix and time-contour representations.

B. Perturbation expansion of the Green's function

The most appreciated feature of the NEGF theory is its perturbation expansion [8] technique for treating many different kinds of complex interactions, such as interaction with electrodes, random impurity scattering, and electron-phonon/photon/electron interactions. In particular, an unknown GF of a system can be expanded to an infinite series with definite calculable quantities. In the presence of some complex interaction, one divides the system Hamiltonian H into two parts

$$H = H_0 + \Sigma, \quad (19)$$

where H_0 refers to an unperturbed Hamiltonian of which the GF can be calculated exactly, and Σ is the self-energy due to the complex interaction in the system. A very important result by using the perturbation expansion is that

$$G = G_0 + G_0\Sigma G_0 + G_0\Sigma G_0\Sigma G_0 + \cdots, \quad (20)$$

where the GF of the realistic system, G, is expanded as an infinite series in terms of G_0 (the GF of the unperturbed Hamiltonian H_0) and Σ. Equation (20) can be rewritten in a more compact form, namely the Dyson equation

$$G = G_0 + G_0\Sigma G = G_0 + G\Sigma G_0, \quad (21)$$

which is satisfied by many GFs, including the retarded/advanced GFs and different representations of the contour-ordered GF [6,8,44]. By replacing quantities with the 2×2 real-time matrices, the relations between various real-time GFs in the presence of interaction Σ can be derived from simple matrix multiplication, such as the Keldysh formula [38] in Eq. (3). Equation (21) provides an important basis to treat various complex problems in the NEGF theory, such as the disorder-averaging problem that we want to solve in this paper.

IV. GENERALIZED COHERENT POTENTIAL APPROXIMATION

The conventional CPA formulation [23,24] of the averaged retarded/advanced GFs $\langle G^{R/A} \rangle$ is based on the Dyson equation for $G^{R/A}$, namely Eq. (21). Because of the fact that the contour-ordered GF takes the same form of the perturbation expansion as the retarded/advanced GFs, it is straightforward to extend the conventional CPA formulation to a general case $\langle G \rangle$ which satisfies Eq. (21). In this section, we present a generalized CPA to calculate the disorder average of various GFs introduced in the NEGF theory.

A. Theory of generalized CPA

For the system as shown in Fig. 1(b), because of the unintentional impurities, the potential of the system V is random. V can be written as the contribution from each cell centered on the atomic nucleus, namely $V = \sum_n v_n$, where

v_n is the on-site random potential. The Hamiltonian of this system can be divided into

$$H = H_0 + \Sigma_{ld} + V, \quad (22)$$

where H_0 is a perfect system Hamiltonian and Σ_{ld} is the self-energy due to the leads. The central idea of CPA is to construct a coherent effective medium whose GF $\bar{G}$ is equal to the disorder-averaged GF $\langle G \rangle$ of the system, namely

$$\bar{G} = \langle G \rangle. \quad (23)$$

To physically describe this effective medium, one can introduce a self-energy due to disorders $\Sigma_{im} = \sum_n \Sigma_{im,n}$, which contains contributions from each site, and rewrite the disordered system Hamiltonian as

$$H = (H_0 + \Sigma) + (V - \Sigma_{im}), \quad (24)$$

where $\Sigma = \Sigma_{ld} + \Sigma_{im}$ contains the contributions from both the leads and effective medium. The term in the first set of parentheses in Eq. (24) can be regarded as the Hamiltonian of the effective medium and the second set of parentheses contain the deviation of the random potential from Σ_{im} which can be rewritten as

$$V - \Sigma_{im} = \sum_n (v_n - \Sigma_{n,im}). \quad (25)$$

With the perturbation expansion technique of the GF, one can obtain the following two Dyson equations:

$$G = \bar{G} + \bar{G}(V - \Sigma_{im})G = \bar{G} + G(V - \Sigma_{im})\bar{G}, \quad (26)$$

$$\bar{G} = G_0 + G_0 \Sigma \bar{G} = G_0 + \bar{G} \Sigma G_0, \quad (27)$$

where G, $\bar{G}$, and G_0 are the GFs corresponding to the Hamiltonians H, $H_0 + \Sigma$, and H_0, respectively. Here, Eq. (26) can be rewritten in another form,

$$G = \bar{G} + \bar{G} T \bar{G}, \quad (28)$$

where T is called the T matrix defined as

$$\begin{aligned} T &\equiv (V - \Sigma_{im}) + (V - \Sigma_{im})\bar{G}(V - \Sigma_{im}) + \cdots \\ &= (V - \Sigma_{im})(I + \bar{G}T) = (I + T\bar{G})(V - \Sigma_{im}). \end{aligned} \quad (29)$$

From Eq. (28), we can see that the T matrix contains all the complexities of a disordered device. By taking the average on both sides of Eq. (28) and comparing with Eq. (23), one finds an important equation,

$$\langle T \rangle = 0, \quad (30)$$

namely the CPA condition for the effective medium Σ_{im} [23,24]. In principle, the above equation in combination with Eq. (27) provides a closed set of self-consistent equations to solve Σ_{im} and $\bar{G}$ of the effective medium. However, to evaluate $\langle T \rangle$ in Eq. (30), one needs to enumerate all possible configurations of the disorders, which is computationally prohibitive. Therefore, further approximation to the average of the T matrix is required to enable CPA self-consistent calculation.

B. Single-site approximation

In order to make Eq. (30) practically useful, the single-site approximation (SSA) [45] was introduced to decouple all the disorder scattering events contained in the T. To formulate SSA, one can insert Eq. (25) into Eq. (29) and get

$$T = \sum_n (v_n - \Sigma_{n,im})(I + \bar{G}T) \equiv \sum_n Q_n, \quad (31)$$

where $Q_n \equiv (v_n - \Sigma_{n,im})(I + \bar{G}T)$ can be solved to obtain

$$Q_n = t_n \left(I + \bar{G} \sum_{m \neq n} Q_m \right), \quad (32)$$

$$t_n \equiv [I - (v_n - \Sigma_{n,im})\bar{G}]^{-1}(v_n - \Sigma_{n,im}). \quad (33)$$

Here, t_n describes the scattering event on the single site n ($t_n = 0$ at the site without random occupations). By recursively substituting Eq. (32) into Eq. (31), we get the multiple scattering equation:

$$T = \sum_n t_n + \sum_{n \neq m} \sum_m t_n \bar{G} t_m + \cdots. \quad (34)$$

From this equation, we can see that the overall disorder scattering effects during electron transport are regarded as successive multiple scattering processes from one site to another. For example, the first two terms in Eq. (34) are contributed by the respective one-time and two-time scattering processes. From Eq. (34), we can also see that the process in which an electron is successively scattered twice on the same site is prohibited. Averaging Eq. (34) gives

$$\langle T \rangle = \sum_n \langle t_n \rangle + \sum_{n \neq m} \langle t_n \bar{G} t_m \rangle + \cdots. \quad (35)$$

At this point, all the formulations are exact. To introduce the SSA, we take the disorder average on Eq. (32) and rewrite it as

$$\langle Q_n \rangle = \langle t_n \rangle \left(I + \bar{G} \sum_{m \neq n} \langle Q_m \rangle \right) + \left\langle t_n \bar{G} \sum_{m \neq n} (Q_m - \langle Q_m \rangle) \right\rangle,$$

where the first term describes the averaged wave scattered by the individual atom on site R, and the second term contains fluctuations away from the average wave. Neglecting the second term yields the SSA, namely

$$\langle Q_n \rangle = \langle t_n \rangle \left(I + \bar{G} \sum_{m \neq n} \langle Q_m \rangle \right), \quad (36)$$

which means that the successive scattering events are independent of each other. Since the probability is small for scattering off multiple impurities at the same time, the SSA is a good approximation and becomes accurate at low impurity concentration.

After applying SSA, we can rewrite Eq. (35) in the following form:

$$\langle T \rangle = \sum_n \langle Q_n \rangle = \sum_n \langle t_n \rangle + \sum_{n \neq m} \langle t_n \rangle \bar{G} \langle t_m \rangle + \cdots. \quad (37)$$

As an immediate result, the CPA self-consistent condition $\langle T \rangle = 0$ is simplified to

$$\langle t_n \rangle \equiv \sum_Q c_n^Q t_n^Q = 0, \tag{38}$$

where c_n^Q is the concentration of the Q element on the site n. Combining the above single-site equation and Eq. (27), the on-site self-energy $\Sigma_{n,im}$ can be self-consistently solved for each site of the system. In such a way, the effective medium described by $\Sigma_{im} = \sum_n \Sigma_{n,im}$ can be efficiently obtained.

C. Application to the Keldysh representation

The quantities we defined so far in the generalized CPA with SSA (such as G, Σ, V, T and their single-site counterparts) are all defined for a general case of GF. If we substitute with the retarded/advanced quantities, we obtain the conventional CPA formalism. Here, we apply the generalized CPA to the Keldysh real-time matrix representation of contour-ordered GF, aiming to obtain the disorder average of all the real-time GFs introduced in Sec. III. To do this, we need to rewrite the quantities G, Σ, V, T and their single-site counterparts in the form of the Keldysh matrix in Eq. (18). For example, $\Sigma = \begin{pmatrix} \Sigma^A & 0 \\ \Sigma^K & \Sigma^R \end{pmatrix}$, $T = \begin{pmatrix} T^A & 0 \\ T^K & T^R \end{pmatrix}$, and $V = \begin{pmatrix} v^A & 0 \\ v^K & v^R \end{pmatrix} = \begin{pmatrix} v & 0 \\ 0 & v \end{pmatrix}$ since the potential is Hermitian. Replacing the quantities in Eq. (27) with Keldysh matrices leads to the following equations (see more details in Appendix B):

$$\bar{G}^R = G_0^R \left(I - \Sigma^R G_0^R \right)^{-1}, \tag{39a}$$

$$\bar{G}^A = G_0^A \left(I - \Sigma^A G_0^A \right)^{-1}, \tag{39b}$$

$$\bar{G}^K = \bar{G}^R \Sigma^K \bar{G}^A + (I + \bar{G}^R \Sigma^R) G_0^K (I + \Sigma^A \bar{G}^A), \tag{39c}$$

where $\Sigma = \Sigma_{ld} + \Sigma_{im}$. Equations (39a) and (39b) for retarded and advanced GFs are the same as the conventional CPA. Equation (39c) is usually called the Keldysh formula for G^K which relates $\bar{G}^K$ to $\bar{G}^{R/A}$ and different components of Σ. From the above equation, we can see the three components of G, namely $G^{R/A/K}$, are not independent of each other: G^A is the conjugate of G^R, and thus G^K is given by G^R through the Keldysh formula. Thus G^R provides sufficient knowledge to compute NEGFs, provided the self-energy Σ. This fact forms the important physical foundation for the CPA-NVC method [22] in which the conventional CPA is carried out only for $\bar{G}^{R/A}$. Actually, the similar relations between the retarded/advanced and the Keldysh quantities can also be found for other quantities, such as T and t_n, as we show in the following.

To obtain the CPA equations, we apply the Keldysh matrices to Eq. (29), and find

$$T^R = \left[I - \left(V - \Sigma_{im}^R \right) \bar{G}^R \right]^{-1} \left(V - \Sigma_{im}^R \right), \tag{40a}$$

$$T^A = \left[I - \left(V - \Sigma_{im}^A \right) \bar{G}^A \right]^{-1} \left(V - \Sigma_{im}^A \right), \tag{40b}$$

$$T^K = T^R \bar{G}^K T^A - (I + T^R \bar{G}^R) \Sigma_{im}^K (I + \bar{G}^A T^A). \tag{40c}$$

Similarly, applying the Keldysh matrices to Eq. (33) directly leads to

$$t_n^R = \left[I - \left(v_n - \Sigma_{n,im}^R \right) \bar{G}^R \right]^{-1} \left(v_n - \Sigma_{n,im}^R \right), \tag{41a}$$

$$t_n^A = \left[I - \left(v_n - \Sigma_{n,im}^A \right) \bar{G}^A \right]^{-1} \left(v_n - \Sigma_{n,im}^A \right), \tag{41b}$$

$$t_n^K = t_n^R \bar{G}^K t_n^A - \left(I + t_n^R \bar{G}^R \right) \Sigma_{n,im}^K \left(I + \bar{G}^A t_n^A \right). \tag{41c}$$

The quantity Σ_{im}^K in Eqs. (40c) and (41c) is called the nonequilibrium coherent potential in the literature of NECPA [35,36]. We provide a simple proof that Σ_{im}^K is generally equal to the NVC [22] in Appendix E. Here Eqs. (40c) and (41c) can be called the Keldysh formula for T and t_n. Similarly to G, we find that the retarded, advanced, and Keldysh components of T or t_n are also not independent. After applying to the Keldysh representation, by combining Eqs. (39) and (41) with the CPA condition $\langle t_n^{R/A/K} \rangle = 0$ in SSA, we can self-consistently compute the self-energy $\Sigma_{im}^{R/A/K}$ and $\bar{G}^{R/A/K}$ to obtain the effective medium. As an important result, according to the relations in Appendix C, the average of all other real-time GFs can be easily obtained with the linear combination of the averaged $\bar{G}^{R/A/K}$.

V. GENERALIZED NONEQUILIBRIUM VERTEX CORRECTION

The generalized CPA only provides an effective way to average a single GF. However, many physical quantities contain the product of two GFs, such as all the quantum transport properties mentioned in Sec. II. Because the two GFs describing the same disordered system are internally correlated by the multiple disorder scattering, $\langle GCG \rangle$ is not simply equal to $\langle G \rangle C \langle G \rangle$ where C is an arbitrary constant. In this section, the generalized NVC is formulated to compute $\langle GCG \rangle$, so that the disorder average of any two-GF correlator can be obtained, such as $\langle G^< C G^< \rangle$.

A. Theory of generalized nonequilibrium vertex correction

Here, we consider a two-GF correlator

$$K = \langle G(z_1) C G(z_2) \rangle, \tag{42}$$

where C is an arbitrary constant. In Eq. (42), the GFs can be at two different energies. For simplicity, these energy indices will be suppressed in the rest of the derivation. To evaluate K, we insert Eq. (28) into Eq. (42) and apply the CPA condition $\langle T \rangle = 0$, and then obtain

$$\langle GCG \rangle = \bar{G}(C + \Omega) \bar{G}, \tag{43}$$

where

$$\Omega \equiv \langle T \bar{G} C \bar{G} T \rangle \tag{44}$$

is the generalized NVC, containing all the effects of disorders on the two-GF correlator.

In order to compute Ω, one can substitute the T with Eq. (31) and then obtain

$$\Omega = \sum_n \sum_m \langle Q_n \bar{G} C \bar{G} \tilde{Q}_m \rangle. \tag{45}$$
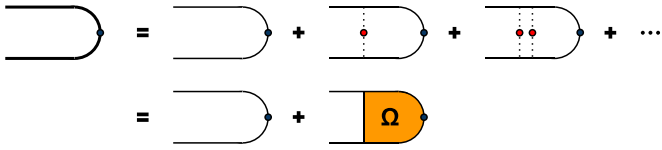
FIG. 3. Diagrammatic representation of $\langle GCG \rangle$. The thick line and thin line represent G and $\bar{G}$, respectively. The dashed line represents the interaction with the disorders (red dots). The blue dot represents a vertex C.

For terms with $n \neq m$, by applying SSA, we can obtain $\langle Q_n \bar{G} C \bar{G} \tilde{Q}_m \rangle = 0$. Consequently, Eq. (45) is simplified to

$$\Omega = \sum_n \Omega_n, \qquad (46)$$

where we have defined $\Omega_n \equiv \langle Q_n \bar{G} C \bar{G} \tilde{Q}_n \rangle$. To proceed further, we replace the Q_n, $\tilde{Q}_n$ with the relation in Eq. (32), $Q_n = t_n(I + \bar{G} \sum_{p \neq n} Q_p)$ and its counterpart $\tilde{Q}_n = (I + \sum_{q \neq n} \tilde{Q}_q \bar{G}) t_n$, and get

$$\Omega_n = \left\langle t_n \left(I + \bar{G} \sum_{p \neq n} Q_p \right) \bar{G} C \bar{G} \left(I + \sum_{q \neq n} \tilde{Q}_q \bar{G} \right) t_n \right\rangle. \qquad (47)$$

Expanding the products in $\langle \cdots \rangle$, one gets four terms, among which, after applying SSA, two terms involving the single Q vanish, and the term involving the product of two Qs is simplified to $\langle t_n \bar{G} \sum_{p \neq n} \Omega_p \bar{G} t_n \rangle$. Therefore, Eq. (47) finally becomes

$$\Omega_n = \langle t_n \bar{G} C \bar{G} t_n \rangle + \sum_{p \neq n} \langle t_n \bar{G} \Omega_p \bar{G} t_n \rangle, \qquad (48)$$

which forms a closed set of linear equations for the unknown Ω_n. In Eq. (48), the average is over pairs of scattering events on the same site. In other words the scattering from different sites is regarded as statistically uncorrelated and the motion of two particles, represented by the two GFs, in the medium is correlated only if they both scatter from the same site. Solving Eq. (48) leads to Ω_n for each disordered site, and thus the averaged two-GF correlator in Eq. (42) can be obtained. The procedure to average the two-GF correlator from Eq. (43) to Eq. (48) can be represented by the Feynman diagrams as shown in Fig. 3 [46]. The first line in Fig. 3 expresses the two-GF correlator with an infinite series of ladder diagrams that refers to the direct expansion of the GFs in SSA, and the second line reduces the infinite ladder series to a single NVC. With this simple Feynman diagram, the various two-GF correlators, such as $G^< C G^<$, can be calculated in a much more effective way than the diagrammatic technique reported in Ref. [5].

B. Application to the Keldysh representation

Similar to the generalized CPA, the generalized NVC formalism can also be applied to the Keldysh representation. To do so, we first consider the arbitrary constant C matrix for

the following four different cases:

$$C^{(1)} = \begin{pmatrix} C & 0 \\ 0 & 0 \end{pmatrix}, \qquad C^{(2)} = \begin{pmatrix} 0 & C \\ 0 & 0 \end{pmatrix},$$

$$C^{(3)} = \begin{pmatrix} 0 & 0 \\ C & 0 \end{pmatrix}, \qquad C^{(4)} = \begin{pmatrix} 0 & 0 \\ 0 & C \end{pmatrix}.$$

By applying these four $C^{(i)}$s to Eq. (44), we obtain four different $\Omega^{(i)}$s as follows,

$$\Omega^{(1)} = \begin{pmatrix} \Omega^{AA} & 0 \\ \Omega^{KA} & 0 \end{pmatrix}, \quad \Omega^{(2)} = \begin{pmatrix} \Omega^{AK} & \Omega^{AR} \\ \Omega^{KK} & \Omega^{KR} \end{pmatrix},$$

$$\Omega^{(3)} = \begin{pmatrix} 0 & 0 \\ \Omega^{RA} & 0 \end{pmatrix}, \quad \Omega^{(4)} = \begin{pmatrix} 0 & 0 \\ \Omega^{RK} & \Omega^{RR} \end{pmatrix}.$$

Applying these $\Omega^{(i)}$ and the corresponding $C^{(i)}$ to Eq. (43) leads to nine different pairwise combinations of G^R, G^A, and G^K:

$$\langle G^R C G^R \rangle = \bar{G}^R (C + \Omega^{RR}) \bar{G}^R, \qquad (49)$$

$$\langle G^R C G^A \rangle = \bar{G}^R (C + \Omega^{RA}) \bar{G}^A, \qquad (50)$$

$$\langle G^A C G^R \rangle = \bar{G}^A (C + \Omega^{AR}) \bar{G}^R, \qquad (51)$$

$$\langle G^A C G^A \rangle = \bar{G}^A (C + \Omega^{AA}) \bar{G}^A, \qquad (52)$$

$$\langle G^R C G^K \rangle = \bar{G}^R \Omega^{RK} \bar{G}^A + \bar{G}^R (C + \Omega^{RR}) \bar{G}^K, \quad (53)$$

$$\langle G^A C G^K \rangle = \bar{G}^A \Omega^{AK} \bar{G}^A + \bar{G}^A (C + \Omega^{AR}) \bar{G}^K, \quad (54)$$

$$\langle G^K C G^R \rangle = \bar{G}^R \Omega^{KR} \bar{G}^R + \bar{G}^K (C + \Omega^{AR}) \bar{G}^R, \quad (55)$$

$$\langle G^K C G^A \rangle = \bar{G}^R \Omega^{KA} \bar{G}^A + \bar{G}^K (C + \Omega^{AA}) \bar{G}^A, \quad (56)$$

$$\langle G^K C G^K \rangle = \bar{G}^R \Omega^{KK} \bar{G}^A + \bar{G}^K \Omega^{AK} \bar{G}^A$$
$$+ \bar{G}^R \Omega^{KR} \bar{G}^K + \bar{G}^K (C + \Omega^{AR}) \bar{G}^K. \quad (57)$$

With the linear combination of these nine quantities, one can obtain the average of any two-GF correlators (see Appendix C for more details). For example:

$$\langle G^< C G^< \rangle = \frac{1}{4} [\langle G^R C G^R \rangle - \langle G^R C G^A \rangle - \langle G^R C G^K \rangle$$
$$- \langle G^A C G^R \rangle + \langle G^A C G^A \rangle + \langle G^A C G^K \rangle$$
$$- \langle G^K C G^R \rangle + \langle G^K C G^A \rangle + \langle G^K C G^K \rangle]. \qquad (58)$$

The remaining task is to find the nine generalized NVC quantities defined in the four $\Omega^{(i)}$s. By inserting the Keldysh matrices into Eq. (48), we obtain nine linear equations with details provided in Appendix D. From Appendix D, by solving the nine equations from top to bottom, we can obtain the nine generalized NVCs to account for the multiple impurity scattering under the nonequilibrium condition. Consequently, with the generalized NVC, the averaged physical properties which contain two-Green's-function correlators, such as averaged nonequilibrium electron density, averaged current, current fluctuation, and averaged shot noise (see Sec. II), can all be computed in a unified way. The nine NVCs are the major results of this work.
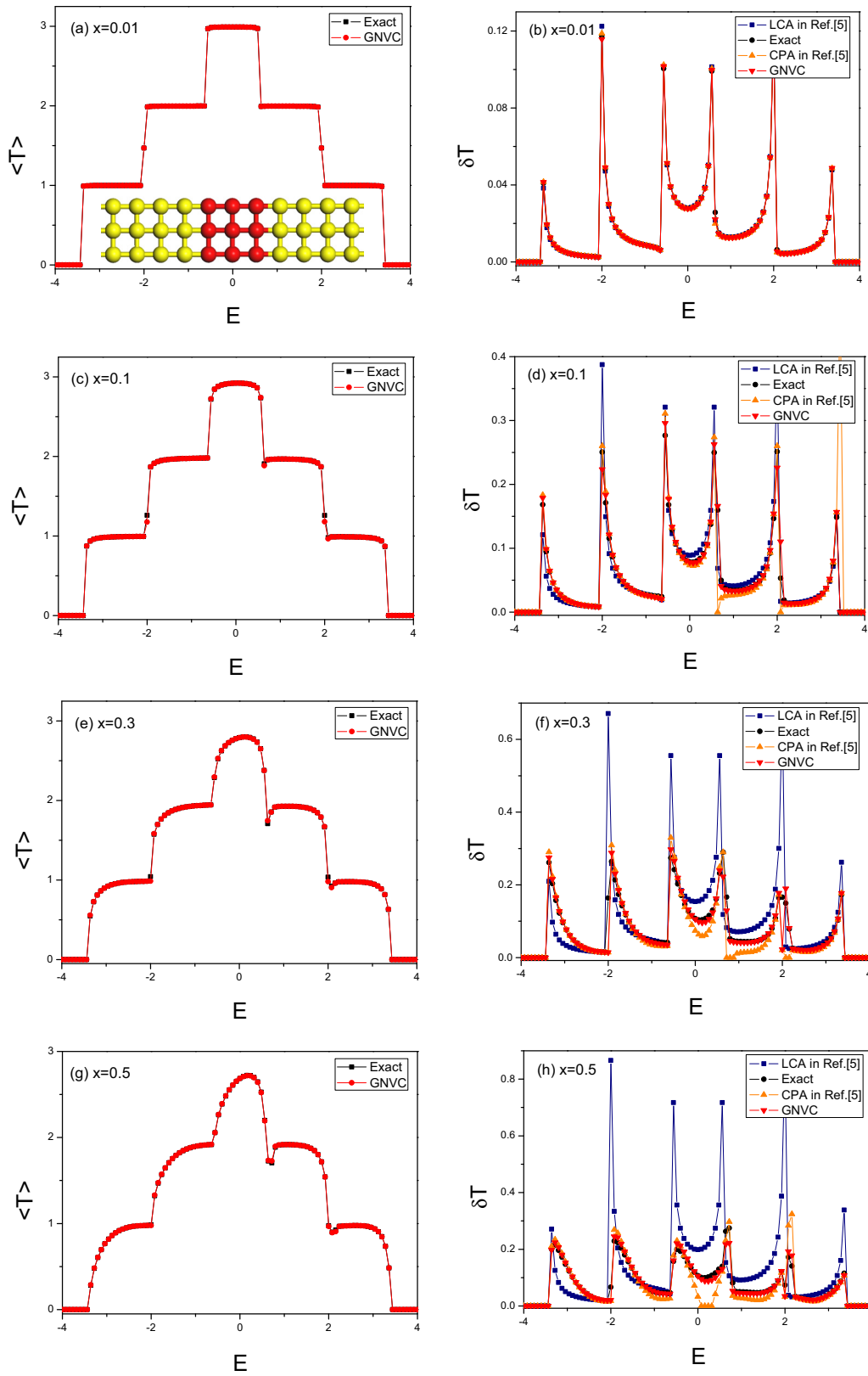
FIG. 4. Numerical results of a nanoribbon with a lattice tight-binding model containing 3×3 disordered sites as shown in inset of (a). The left column—(a), (c), (e), and (g)—and the right column—(b), (d), (f), and (h)—show the averaged transmission coefficients and the corresponding fluctuations with disorder concentrations $x = 0.01, 0.1, 0.3, 0.5$, respectively.

VI. NUMERICAL RESULTS AND DISCUSSION

To validate the generalized CPA-NVC formalism, we use the same square-lattice tight-binding model as in Ref. [5] to calculate the averaged transmission $\langle T \rangle$ and its fluctuation δT. As shown in the inset of Fig. 4(a), the central scattering region contains disordered 3×3 lattice sites (red color), of which each is occupied by the host atom whose on-site energies $v = 0$ with probability $1 - x$, or occupied by the impurity atom whose on-site energy $v_{im} = 0.5$ with probability x. The two semi-infinite leads are assumed to be perfect with the on-site energies equal to 0. The electron hopping only happens between the first-nearest neighbors with the strength $t = 1$. The exact solution was calculated by enumerating every possible configuration, namely $2^9 = 512$ cases, and then weighted by the probabilities.

The left column of Fig. 4, namely panels (a), (c), (e), and (g), shows the averaged transmission of the model for different concentrations of impurities. Theoretically, in a perfect system, the transmission is a steplike curve with the value equal to the number of modes at that energy. As the impurity concentration increases, the transmission curve becomes smooth because of the interchannel scattering by disordered impurities as shown in Fig. 4. We can see the averaged transmissions calculated by our generalized NVC for all concentrations are all very close to the exact results, providing a good validation to our NVC formalism for calculating $\langle G^< \rangle = \langle G^R \Sigma^< G^A \rangle$. To further test the generalized NVCs, the right column of Fig. 4, namely panels (b), (d), (f), and (h), shows the transmission fluctuation for different concentrations of disorder. Besides the exact results and our generalized NVC calculations, we also plot the results of the low concentration limit (LCA) and CPA based diagrammatic techniques reported in Ref. [5] for comparison. We can see in the low impurity concentration, e.g., $x = 0.01$, all three approximate methods perform quite well in comparison with the exact results. However, when the disorder concentration increases, both LCA and CPA based diagrammatic techniques [5] become less and less accurate. In particular, one can find the large errors in LCA results in Figs. 4(d), 4(f), and 4(h), and at the same time the diagrammatic technique even produces unphysical results at some energy regions (δT is a negative value and has been set to zero in the plots). However, the generalized NVC calculations agree very well with the exact results for all the disorder concentrations, even at $x = 0.5$. This agreement provides an important test of the general applicability of the generalized CPA-NVC method. Thus we believe the generalized CPA-NVC formalism provides an effective way for simulating disordered nanoelectronics.

VII. CONDITIONALLY AVERAGED GREEN'S FUNCTION

In previous sections, we have introduced the generalized CPA-NVC algorithm to treat the disorder effects in quantum transport. In this section, we will discuss how to combine the generalized CPA-NVC with the NEGF-DFT method to calculate the electronic structure of the disordered nanoelectronics from first principles.

The central quantity for realizing DFT self-consistent calculation is the conditionally averaged lesser Green's function
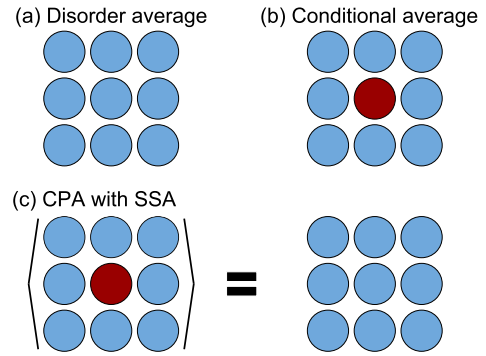
FIG. 5. (a) A fully disorder averaged system. (b) A conditionally averaged system. (c) Schematic illustration of CPA with SSA.

$\bar{G}^{<,Q}$, which gives the ρ_n^Q to update v_n^Q in each DFT iteration. In general, the conditionally averaged GF $\bar{G}^Q$ is associated with the system in which the nth site is occupied by the fixed Q element, and the disorder average is carried out for the rest of the disordered sites. Thus, $\bar{G}^Q$ corresponds to the effective medium with the Q element occupying the site n, as shown in Fig. 5(b).

In order to calculate $\bar{G}^Q$, we expand it with reference to $\bar{G}$ shown in Fig. 5(a) by using Eq. (28), and obtain

$$\bar{G}^Q = \bar{G} + \bar{G} t_n^Q \bar{G}, \tag{59}$$

where

$$t_n^Q = \left[I - \left(v_n^Q - \Sigma_{n,im} \right) \bar{G} \right]^{-1} \left(v_n^Q - \Sigma_{n,im} \right). \tag{60}$$

Note that we have used $T = t_n^Q$ since there is only one scattering center. One can check that

$$\sum_Q c^Q \bar{G}^Q = \bar{G} \tag{61}$$

by applying the single-site CPA condition $\langle t_n \rangle = 0$ in Eq. (59). Figure 5(c) provides a schematic illustration of the above equation. By substituting with Keldysh matrices in Eq. (59), we obtain

$$\bar{G}^{R,Q} = \bar{G}^R + \bar{G}^R t_n^{R,Q} \bar{G}^R, \tag{62a}$$

$$\bar{G}^{A,Q} = \bar{G}^A + \bar{G}^A t_n^{A,Q} \bar{G}^A, \tag{62b}$$

$$\begin{aligned} \bar{G}^{K,Q} = {} & \bar{G}^K + \bar{G}^R t_n^{K,Q} \bar{G}^A \\ & + \bar{G}^K t_n^{A,Q} \bar{G}^A + \bar{G}^R t_n^{R,Q} \bar{G}^K, \end{aligned} \tag{62c}$$

where the matrices $t_n^{R/A/K}$ are defined in Eq. (41). With the above three conditionally averaged GFs, $\bar{G}^{<,Q}$ can be calculated by the relation

$$\bar{G}^{<,Q} = \tfrac{1}{2}(-\bar{G}^{R,Q} + \bar{G}^{A,Q} + \bar{G}^{K,Q}). \tag{63}$$

The conditionally averaged $\bar{G}^{<,Q}$ provides the nonequilibrium density matrix $\bar{\rho}^Q$ for each disordered element in the system. In combination with DFT, the potential v_n^Q can be computed from the electron density in a self-consistent way. As a result, the effects of disorders on the quantum transport properties can be simulated from first principles.

VIII. CONCLUSIONS

We have developed a generalized CPA-NVC formalism to realize quantum transport simulation of disordered nano-electronic devices at nonequilibrium states. The generalized CPA-NVC formalism provides an effective way to compute the disorder average of any two-GF correlator. We obtain nine NVCs to account for the effects of the multiple impurity scattering under nonequilibrium conditions. As an important result, various nonequilibrium quantum transport properties, including the averaged nonequilibrium density matrix, averaged current, current fluctuation, and averaged shot noise, can all be effectively derived and computed with the nine NVCs. To test the general applicability of the generalized CPA-NVC method, we have applied it to calculate the transmission coefficient and its fluctuation with a tight-binding model and found our calculations agree well with the exact results for a wide range of disorder concentrations and energies. In addition, the general form of the conditionally averaged NEGF is also derived to combine with DFT to enable first-principles simulation of disordered nanoelectronics. As a summary, the generalized CPA-NVC method provides a unified, effective, and general approach for simulating nonequilibrium quantum transport through disordered nanoelectronics.

ACKNOWLEDGMENTS

APPENDIX A: RELATIONS BETWEEN ANALYTICAL CONTINUATION WITH THE LANGRETH THEOREM AND THE MATRIX REPRESENTATION

The operation on contour-ordered quantities requires integration along the time contour, which can be transformed into integration along the real-time axis by using the Langreth theorem [8]. For example, suppose A, B, and D are three quantities defined on the contour and have the relation

$$D = AB. \tag{A1}$$

According to the Langreth theorem, their real-time counterparts have the relations

$$D^< = A^R B^< + A^< B^A, \tag{A2}$$

$$D^R = A^R B^R. \tag{A3}$$

These two identities can be derived by deforming the time contour as indicated in Fig. 4.4 in Ref. [8]. An alternative way to apply the Langreth theorem is by using the Craig or Keldysh 2×2 real-time matrix representation of the contour-ordered quantities. For example, by substituting the matrix notation defined in (17) into (A1), we obtain

$$\begin{pmatrix} D^t & -D^< \\ D^> & -D^{\bar{t}} \end{pmatrix} = \begin{pmatrix} A^t B^t - A^< B^> & -A^t B^< + A^< B^{\bar{t}} \\ A^> B^t - A^{\bar{t}} B^> & -A^> B^< + A^{\bar{t}} B^{\bar{t}} \end{pmatrix}.$$

From this expression, we directly recover (A2),

$$D^< = A^t B^< - A^< B^{\bar{t}}$$
$$= (A^t - A^<)B^< + A^<(B^< - B^{\bar{t}}) = A^R B^< + A^< A^A.$$

Similarly, substituting Eq. (18) into Eq. (A1) leads to Eq. (A3). Therefore, we can regard these 2×2 matrices as inherently incorporating the Langreth theorem and they are preferred in practical applications in this paper.

APPENDIX B: DERIVATION OF EQUATION (39)

We first rewrite Eq. (27) for $\bar{G}$

$$\bar{G} = G_0(I - \Sigma G_0)^{-1}. \tag{B1}$$

By replacing with the Keldysh representation defined in Eq. (18), we obtain

$$\begin{pmatrix} \bar{G}^A & 0 \\ \bar{G}^K & \bar{G}^R \end{pmatrix} = \begin{pmatrix} G_0^A & 0 \\ G_0^K & G_0^R \end{pmatrix} \begin{pmatrix} A & 0 \\ K & R \end{pmatrix}^{-1}, \tag{B2}$$

where we have defined

$$R \equiv I - \Sigma^R G_0^R, \tag{B3}$$

$$A \equiv I - \Sigma^A G_0^A, \tag{B4}$$

$$K \equiv -\Sigma^K G_0^A - \Sigma^R G_0^K. \tag{B5}$$

Using the identity

$$\begin{pmatrix} A & 0 \\ K & R \end{pmatrix}^{-1} = \begin{pmatrix} A^{-1} & 0 \\ -R^{-1} K A^{-1} & R^{-1} \end{pmatrix}, \tag{B6}$$

then we can get

$$\bar{G}^R = G_0^R R^{-1} = G_0^R \big[I - \Sigma^R G_0^R \big]^{-1}, \tag{B7a}$$

$$\bar{G}^A = G_0^A A^{-1} = G_0^A \big[I - \Sigma^A G_0^A \big]^{-1}, \tag{B7b}$$

$$\bar{G}^K = G_0^K A^{-1} - G_0^R R^{-1} K A^{-1}$$
$$= \bar{G}^R \Sigma^K \bar{G}^A + (I + \bar{G}^R \Sigma^R) G_0^K (G_0^A)^{-1} \bar{G}^A$$
$$= \bar{G}^R \Sigma^K \bar{G}^A + (I + \bar{G}^R \Sigma^R) G_0^K (I + \Sigma^A \bar{G}^A). \tag{B7c}$$

APPENDIX C: EXPRESSING VARIOUS REAL-TIME QUANTITIES IN TERMS OF Q^R, Q^A, AND Q^K

This appendix provides a convenient way to express the various real-time quantities in terms of the linear combinations of Q^R, Q^A, and Q^K by using the Keldysh linear transformation shown as follows:

$$\begin{pmatrix} Q^t & -Q^< \\ Q^> & -Q^{\bar{t}} \end{pmatrix} = \frac{1}{2} \begin{pmatrix} 1 & 1 \\ -1 & 1 \end{pmatrix} \begin{pmatrix} Q^A & 0 \\ Q^K & Q^R \end{pmatrix} \begin{pmatrix} 1 & -1 \\ 1 & 1 \end{pmatrix}$$
$$= \frac{1}{2} \begin{pmatrix} Q^R + Q^A + Q^K & Q^R - Q^A - Q^K \\ Q^R - Q^A + Q^K & Q^R + Q^A - Q^K \end{pmatrix}.$$

Furthermore, if we want to express the various pairwise combinations of real-time quantities, for example $Q^< C Q^<$, we can just substitute $Q^< = (-Q^R + Q^A + Q^K)/2$ into $Q^< C Q^<$ and expand it into nine terms involving $Q^{R/A/K} C Q^{R/A/K}$.

APPENDIX D: NINE EQUATIONS FOR THE GENERALIZED NVCs

The following nine equations are obtained from Eq. (48) in the Keldysh representation with four cases of $C^{(i)}$ and $\Omega^{(i)}$ ($i = 1,2,3,4$):

$$\Omega_n^{RR} = \langle t_n^R \bar{G}^R C \bar{G}^R t_n^R \rangle + \sum_{p \neq n} \langle t_n^R \bar{G}^R \Omega_p^{RR} \bar{G}^R t_n^R \rangle, \tag{D1}$$

$$\Omega_n^{RA} = \langle t_n^R \bar{G}^R C \bar{G}^A t_n^A \rangle + \sum_{p \neq n} \langle t_n^R \bar{G}^R \Omega_p^{RA} \bar{G}^A t_n^A \rangle, \tag{D2}$$

$$\Omega_n^{AR} = \langle t_n^A \bar{G}^A C \bar{G}^R t_n^R \rangle + \sum_{p \neq n} \langle t_n^A \bar{G}^A \Omega_p^{AR} \bar{G}^R t_n^R \rangle, \tag{D3}$$

$$\Omega_n^{AA} = \langle t_n^A \bar{G}^A C \bar{G}^A t_n^A \rangle + \sum_{p \neq n} \langle t_n^A \bar{G}^A \Omega_p^{AA} \bar{G}^A t_n^A \rangle, \tag{D4}$$

$$\Omega_n^{RK} = \langle t_n^R \bar{G}^R C \bar{G}^R t_n^K \rangle + \langle t_n^R \bar{G}^R C \bar{G}^K t_n^A \rangle + \sum_{p \neq n} [\langle t_n^R \bar{G}^R \Omega_p^{RK} \bar{G}^A t_n^A \rangle + \langle t_n^R \bar{G}^R \Omega_p^{RR} \bar{G}^R t_n^K \rangle + \langle t_n^R \bar{G}^R \Omega_p^{RR} \bar{G}^K t_n^A \rangle], \tag{D5}$$

$$\Omega_n^{AK} = \langle t_n^A \bar{G}^A C \bar{G}^R t_n^K \rangle + \langle t_n^A \bar{G}^A C \bar{G}^K t_n^A \rangle + \sum_{p \neq n} [\langle t_n^A \bar{G}^A \Omega_p^{AK} \bar{G}^A t_n^A \rangle + \langle t_n^A \bar{G}^A \Omega_p^{AR} \bar{G}^R t_n^K \rangle + \langle t_n^A \bar{G}^A \Omega_p^{AR} \bar{G}^K t_n^A \rangle], \tag{D6}$$

$$\Omega_n^{KR} = \langle t_n^K \bar{G}^A C \bar{G}^R t_n^R \rangle + \langle t_n^R \bar{G}^K C \bar{G}^R t_n^R \rangle + \sum_{p \neq n} [\langle t_n^R \bar{G}^R \Omega_p^{KR} \bar{G}^R t_n^R \rangle + \langle t_n^K \bar{G}^A \Omega_p^{AR} \bar{G}^R t_n^R \rangle + \langle t_n^R \bar{G}^K \Omega_p^{AR} \bar{G}^R t_n^R \rangle], \tag{D7}$$

$$\Omega_n^{KA} = \langle t_n^K \bar{G}^A C \bar{G}^A t_n^A \rangle + \langle t_n^R \bar{G}^K C \bar{G}^A t_n^A \rangle + \sum_{p \neq n} [\langle t_n^R \bar{G}^R \Omega_p^{KA} \bar{G}^A t_n^A \rangle + \langle t_n^K \bar{G}^A \Omega_p^{AA} \bar{G}^A t_n^A \rangle + \langle t_n^R \bar{G}^K \Omega_p^{AA} \bar{G}^A t_n^A \rangle], \tag{D8}$$

$$\Omega_n^{KK} = \langle t_n^K \bar{G}^A C \bar{G}^R t_n^K \rangle + \langle t_n^K \bar{G}^A C \bar{G}^K t_n^A \rangle + \langle t_n^R \bar{G}^K C \bar{G}^R t_n^K \rangle + \langle t_n^R \bar{G}^K C \bar{G}^K t_n^A \rangle$$
$$+ \sum_{p \neq n} [\langle t_n^R \bar{G}^R \Omega_p^{KK} \bar{G}^A t_n^A \rangle + \langle t_n^K \bar{G}^A \Omega_p^{AK} \bar{G}^A t_n^A \rangle + \langle t_n^R \bar{G}^K \Omega_p^{AK} \bar{G}^A t_n^A \rangle + \langle t_n^R \bar{G}^R \Omega_p^{KR} \bar{G}^R t_n^K \rangle$$
$$+ \langle t_n^K \bar{G}^A \Omega_p^{AR} \bar{G}^R t_n^K \rangle + \langle t_n^R \bar{G}^K \Omega_p^{AR} \bar{G}^R t_n^K \rangle + \langle t_n^R \bar{G}^R \Omega_p^{KR} \bar{G}^K t_n^A \rangle + \langle t_n^K \bar{G}^A \Omega_p^{AR} \bar{G}^K t_n^A \rangle + \langle t_n^R \bar{G}^K \Omega_p^{AR} \bar{G}^K t_n^A \rangle]. \tag{D9}$$

APPENDIX E: RELATION BETWEEN NECPA AND CPA-NVC

In this appendix, we will see that the nonequilibrium coherent potential defined in the NECPA [35,36], namely Σ_{im}^K in Eq. (41c), equals the NVC in Ref. [22] or the Ω^{RA} in Eq. (D2) in this paper. To do so, we first consider the Keldysh formula in Eq. (39c), and it can be simplified as follows for a device in steady state:

$$\bar{G}^K = \bar{G}^R \Sigma^K \bar{G}^A, \tag{E1}$$

because the second term in Eq. (39c) equals zero in the steady-state condition [7,47]. By substituting Eq. (E1) into

(40c) and using the CPA condition of Eq. (30), we obtain the nonequilibrium coherent potential in the following form:

$$\Sigma_{im}^K = \langle T^R \bar{G}^R \Sigma_{ld}^K \bar{G}^A T^A \rangle, \tag{E2}$$

which is exactly the same as the NVC in Eq. (44). Applying the SSA still does not change the conclusion. In particular, applying $\langle t_n^K \rangle = 0$ to Eq. (41c) results in

$$\Sigma_{n,im}^K = \langle t_n^R \bar{G}^R \Sigma_{ld} \bar{G}^A t_n^A \rangle + \sum_{m \neq n} \langle t_n^R \bar{G}^R \Sigma_{m,im}^K \bar{G}^A t_n^A \rangle,$$

which is the same as the NVC formula [22,48] or Eq. (D2). Therefore, we conclude that the method NECPA [35,36] is generally equivalent to the CPA-NVC [22] approach.

[1] T. Markussen, R. Rurali, A.-P. Jauho, and M. Brandbyge, Phys. Rev. Lett. **99**, 076803 (2007).

[2] A. M. Bratkovsky, Phys. Rev. B **56**, 2344 (1997).

[3] H. Ohno, Science **281**, 951 (1998).

[4] A. Asenov, IEEE Trans. Electron Devices **45**, 2505 (1998).

[5] Y. Zhu, L. Liu, and Hong Guo, Phys. Rev. B **88**, 085420 (2013).

[6] L. V. Keldysh, Sov. Phys. JETP **20**, 1018 (1965).

[7] S. Datta, *Electronic Transport in Mesoscopic Systems* (Cambridge University Press, Cambridge, 1997).

[8] H. Haug, A.-P. Jauho, and M. Cardona, *Quantum Kinetics in Transport and Optics of Semiconductors*, Vol. 2 (Springer, Berlin, 2008).

[9] P. Hohenberg and W. Kohn, Phys. Rev. **136**, B864 (1964).

[10] W. Kohn and L. J. Sham, Phys. Rev. **140**, A1133 (1965).

[11] R. G. Parr and W. Yang, *Density-Functional Theory of Atoms and Molecules* (Oxford University Press, Netherlands, 1989).

[12] J. Taylor, H. Guo, and J. Wang, Phys. Rev. B **63**, 121104 (2001).

[13] J. Taylor, H. Guo, and J. Wang, Phys. Rev. B **63**, 245407 (2001).

[14] S. V. Faleev, F. Leonard, D. A. Stewart, and M. van Schilfgaarde, Phys. Rev. B **71**, 195422 (2005).

[15] D. Waldron, P. Haney, B. Larade, A. MacDonald, and H. Guo, Phys. Rev. Lett. **96**, 166804 (2006).

[16] Y. Xue, S. Datta, and M. A. Ratner, J. Chem. Phys. **115**, 4292 (2001).

[17] Y. Xue, S. Datta, and M. A. Ratner, Chem. Phys. **281**, 151 (2002).

[18] M. Brandbyge, J.-L. Mozos, P. Ordejón, J. Taylor, and K. Stokbro, Phys. Rev. B **65**, 165401 (2002).

[19] S.-H. Ke, H. U. Baranger, and W. Yang, Phys. Rev. B **70**, 085410 (2004).

[20] A. R. Rocha, V. M. Garcia-Suarez, S. W. Bailey, C. J. Lambert, J. Ferrer, and S. Sanvito, Nat. Mater. **4**, 335 (2005).

[21] W. Lu, V. Meunier, and J. Bernholc, Phys. Rev. Lett. **95**, 206805 (2005).

[22] Y. Ke, K. Xia, and H. Guo, Phys. Rev. Lett. **100**, 166805 (2008).

[23] P. Soven, Phys. Rev. **156**, 809 (1967).

[24] D. W. Taylor, Phys. Rev. **156**, 1017 (1967).

[25] Y. Ke, K. Xia, and H. Guo, Phys. Rev. Lett. **105**, 236801 (2010).

[26] Y. Ke, F. Zahid, V. Timoshevskii, K. Xia, D. Gall, and H. Guo, Phys. Rev. B **79**, 155406 (2009).

[27] F. Zahid, Y. Ke, D. Gall, and H. Guo, Phys. Rev. B **81**, 045406 (2010).

[28] X. Jia, K. Xia, Y. Ke, and H. Guo, Phys. Rev. B **84**, 014401 (2011).

[29] Z. Wang, Y. Ke, D. Liu, H. Guo, and K. H. Bevan, Appl. Phys. Lett. **101**, 093102 (2012).

[30] J. Maassen and H. Guo, Phys. Rev. Lett. **109**, 266803 (2012).

[31] D. Liu, X. Han, and H. Guo, Phys. Rev. B **85**, 245436 (2012).

[32] C. Heiliger, C. Franz, and M. Czerner, Phys. Rev. B **87**, 224412 (2013).

[33] C. Franz, M. Czerner, and C. Heiliger, Phys. Rev. B **88**, 094421 (2013).

[34] C. Franz, M. Czerner, and C. Heiliger, J. Phys.: Condens. Matter **25**, 425301 (2013).

[35] A. V. Kalitsov, M. G. Chshiev, and J. P. Velev, Phys. Rev. B **85**, 235111 (2012).

[36] Y. Zhu, L. Liu, and H. Guo, Phys. Rev. B **88**, 205415 (2013).

[37] J. N. Zhuang and J. Wang, J. Appl. Phys. **114**, 063708 (2013).

[38] G. D. Mahan, *Many-Particle Physics* (Springer Science & Business Media, New York, 2013).

[39] S. Datta, *Quantum Transport: Atom to Transistor* (Cambridge University Press, Cambridge, 2005).

[40] J. Wang and H. Guo, Phys. Rev. B **79**, 045119 (2009).

[41] M. Büttiker, Phys. Rev. B **46**, 12485 (1992).

[42] Y. Wei, B. Wang, J. Wang, and H. Guo, Phys. Rev. B **60**, 16900 (1999).

[43] E. Lifschitz and L. Pitajewski, in *Textbook of Theoretical Physics* (Akademie Verlag, Berlin, 1983).

[44] R. A. Craig, J. Math. Phys. **9**, 605 (1968).

[45] B. Velický, S. Kirkpatrick, and H. Ehrenreich, Phys. Rev. **175**, 747 (1968).

[46] K. Levin, B. Velický, and H. Ehrenreich, Phys. Rev. B **2**, 1771 (1970).

[47] F. S. Khan, J. H. Davies, and J. W. Wilkins, Phys. Rev. B **36**, 2578 (1987).

[48] B. Velický, Phys. Rev. **184**, 614 (1969).